Textures and Microstructures, 1992, Vol. 19, pp. 101–121
Reprints available directly from the publisher.
Photocopying permitted by license only

DEVELOPMENT OF ROLLING TEXTURES IN AN AUSTENITIC STAINLESS STEEL

C. D. SINGH and V. RAMASWAMY

Research and Development Centre for Iron and Steel, Steel Authority of India Limited, Ranchi-834 002, India

C. SURYANARAYANA

Institute of Materials and Advanced Processes, University of Idaho, Moscow, ID. 83843-4140, USA

(Received June 26, 1991)

Three dimensional texture analysis by means of orientation distribution functions (ODF) was used to examine the texture development during rolling at 473 K in an austenitic stainless steel. With the help of ODFs results, the different stages of texture development could be assigned to the existing theories of heterogeneous deformation mechanisms of low SFE face-centred cubic metals. The texture at very low degree of rolling consists of two limited orientation tubes with their fibre axes ⟨110⟩//ND and ⟨110⟩60°ND and agrees with the predictions made by Taylor model. With further deformation, twinning causes the reduction of ≈{112}⟨111⟩ component and leads to the formation of twin {552}⟨115⟩. Abnormal slip on slip planes parallel to the twin boundaries rotates the twins into the {332}⟨113⟩ and {111}⟨110⟩ positions. The shear bands formation in the rotated twin-matrix lamellae changes their orientations near to {011}⟨100⟩ and {011}⟨112⟩ positions. Finally, normal slip again continues and sharpens the brass-type rolling texture.

KEY WORDS Rolling texture, copper-type, brass-type, slip, mechanical twinning, shear bands

1. INTRODUCTION

The study of the development of rolling textures in cubic metals in general and austenitic stainless steel in particular at ambient temperature, is of great scientific and technological importance, since these control further processing stages and thereby the resulting properties (i.e. Young's modulus or plastic anisotropy). It also gives more information on the active deformation mechanisms in polycrystalline materials.

There is a general consent in the literatures (Wassermann and Grewen, 1962; Lücke, 1981; Bacroix and Jonas, 1988; Hirsch and Lücke, 1988) that face-centred cubic (FCC) metals and alloys possess different rolling texture (i.e. copper-type and brass-type). The transition texture in between copper-type and brass-type is also perceptible. The possible causes for different rolling textures are mainly rolling degree, rolling temperature, starting texture, grain shape and finally the stacking fault energy (SFE). As the SFE increases the texture transition from brass to copper-type takes place and has been systematically surveyed as a function of solute element (Zn) in copper (Alam, Mengelberg and Lücke, 1967) and as a function of rolling temperature in austenitic stainless steel (Goodman

and Hu, 1964), copper (Hu and Goodman, 1963) and silver (Hu and Cline, 1961; Hu, Cline and Goodman, 1961). The FCC rolling textures may be described either in terms of ideal orientations (Hu, Sperry and Beck, 1952) or in terms of complete or limited fibre axis (Grewen and Wassermann, 1955; Wassermann, 1963). According to the concept of ideal orientations, the copper-type texture is characterised mainly by the orientations $\{112\}\langle 111\rangle$, $\{123\}\langle 634\rangle$ and $\{011\}\langle 112\rangle$, in doing so the indexing of $\{123\}\langle 634\rangle$ component can adopt somewhat $\{123\}\langle 412\rangle$ or $\{124\}\langle 211\rangle$, whereas the brass-type texture is dominated by $\{011\}\langle 112\rangle$ and to a lesser extent by $\{011\}\langle 100\rangle$. The transition from copper to brass-type textures is described by the disappearance of $\{112\}\langle 111\rangle$ component. On the contrary, the copper-type texture has been described by taking into consideration not only the ideal orientations $\{112\}\langle 111\rangle$ and $\{011\}\langle 112\rangle$ but also the spread ranges extended between them with the aid of two limited $\langle 111\rangle$ fibres formed by rotations upto $\pm 30°$ about certain $\{111\}$ poles of two ideal components. Out of the two fibre axes, one is taken under 19° to RD on the periphery of the $\{111\}$ pole figure and the other under 19° from ND on the ND/RD radius of the pole figure.

The results obtained from the pole figure analysis were subsequently corroborated after the advent of orientation distribution functions (ODF) technique (Bunge, 1969) by many investigators (Bunge and Tobisch, 1968; Bunge and Haessner, 1968; Bunge, 1971; Davies, Kallend and Ruberg, 1973; Truszkowski *et al.*, 1973; Pospiech and Lücke, 1975; Virnich and Lücke, 1978; Hirsch and Lücke, 1988). According to these investigations, the rolling textures of FCC metals and alloys have been described in terms of two limited fibres (i.e. a fibre axis $\langle 110\rangle$//ND extending from $\{011\}\langle 100\rangle$ to $\{011\}\langle 112\rangle$ and the other fibre $\langle 110\rangle 60°$ND running from $\{112\}\langle 111\rangle$ through $\{123\}\langle 634\rangle$ to $\{011\}\langle 112\rangle$ with $\langle 110\rangle$ axis inclined about 60° from ND towards RD). While the brass-type texture (low SFE materials) is characterised by $\langle 110\rangle$//ND fibre with $\{011\}\langle 112\rangle$ as a major component, the copper-type (high and medium SFE materials) is described mainly by $\langle 110\rangle 60°$ND fibre with $\{112\}\langle 111\rangle$ or $\{123\}\langle 634\rangle$ as major orientation.

Extensive metallographic studies of the deformation structure by optical and transmission electron microscopy (TEM) have been performed on FCC metals like copper and brass and these microscopical results lead to a number of new aspects in the interpretation of deformation structure and texture development (Duggan *et al.*, 1978; Hatherly, 1978; Malin and Hatherly, 1979; Wakefield and Hatherly, 1981). According to Malin and Hatherly (1979) the deformation sequence in high and medium SFE metals (i.e. copper) involves the formation of equiaxed cells, microbands, clustering of microbands and shear bands. In these metals copper-type rolling texture forms which can be determined theoretically from the calculations based on Taylor model (Dillamore, Butler and Green, 1968; Bunge, 1970; Dillamore and Katoh, 1971; Dillamore and Katoh, 1974), Taylor model adapted to both slip and twinning (Van Houtte and Aernoudt, 1976; Van Houtte, 1978a; Van Houtte, 1978b) and relaxed constraints model (Honneff and Mecking, 1981; Van Houtte, 1981). With decrease in SFE, an increasing tendency of mechanical twinning during deformation is often considered as the mechanism (Wassermann, 1963) which causes the change from the copper-type to the brass-type rolling texture. In metals of low SFE such as 70–30 brass (Fargette and Whitwham, 1976; Grewen, Noda and Sauer, 1977; Duggan *et al.*, 1978;

Hutchinson, Duggan and Hatherly, 1979) and stainless steel (Blicharski and Gorczyca, 1978), deformation begins by the glide of partial dislocations, followed by mechanical twinning, the rotation of the twin-parent lamellae into alignment with the rolling plane, the development of shear bands and the resumption of normal octahedral slip in the recovered crystallites of the shear bands. But the effects of the mechanical twinning on further deformation and on the formation of rolling textures in austenitic stainless steel, which become even more complicated by shear band formation, are not yet completely understood. Furthermore, the characterisation of the rolling textures developed in austenitic stainless steel above ambient temperature was based on the pole figure analysis (Goodman and Hu, 1964) which possesses very limited resolving power in revealing the differences which are more of quantitative than of qualitative nature.

The aim of the present investigation was to clarify the microscopical observations of orientations and their statistical appearance in the textures of austenitic stainless steel cold rolled at 473 K by means of the three-dimensional ODF analysis which describes the texture in a more complete, exact and explicit fashion. The results also outline the process of texture development during cold rolling.

2. EXPERIMENTAL PROCEDURE

A commercially produced hot band (HB) of an austenitic stainless steel of nominal composition (by wt%): 19.25% Cr, 8.40% Ni, 0.05% C, 1.24% Mn, 0.48% Si, 0.02% P, 0.02% S was used for the present investigation. As per supplier's information 2.95 mm thick HB strip was finished at about 1173 K and coiled at about 1023 K. In order to remove any oxides and scales from the surfaces, the hot band was pickled in a pickling solution (by volume %) of 10% HNO_3 + 2% HF + 88% distilled water at a temperature 323 K for a period of 5 minutes and then rinsed with water and dried.

The hot band was cold rolled (CR) at a temperature 473 K without lubrication. The cold rolling operation was oriented parallel to the original hot rolling direction and carried out in such a way that the true strain per pass was about 0.05. In the interval between the passes specimens were kept in the furnace at 473 K for a period of 5 minutes in order to maintain the temperature. The two-high mill used had 55 mm dia rollers. The cumulative rolling reductions investigated were from 10 to 90% at intervals of 10%.

Optical metallography was performed on specimen of HB, which was mechanically polished and electrolytically etched in saturated oxalic acid solution at 10 volts for 2 minutes, at section (S = 0) cut perpendicular to the transverse direction containing (R) and normal direction (N) RN. Here S = 0 denotes the mid-thickness of the specimen.

X-ray texture measurements were performed for HB rolled at 0, 30, 50, 70 and 90% reduction in thickness on an automatic texture goniometer, using MoK_α radiation. For each ground and etched specimen (20 mm × 14 mm), the texture was determined at the section (S = 0) parallel to the rolling plane by measuring four incomplete pole figures of the plane {111}, {200}, {220} and {113}, using

Schulz back reflection technique (Schulz, 1949). The diffracted intensity was recorded continuously every 5° along concentric circles in the angular range from 0 to 75° in steps of 5°. The measured intensity was subjected to background, geometrical and defocussing corrections using a random specimen of pressed and sintered austenitic stainless steel powders. Each ODF was calculated from the data of four incomplete pole figures following the series expansion method of Bunge (1982) and using the pseudo-normalisation technique of Kern and Bergmann (1978). The series were extended to the degree $l = 22$. The texture strength as expressed by the texture index J (Truszkowski *et al.*, 1978) which defines the mean square deviation of the ODF from random distribution, was also determined in each case. The inverse pole figure measurements were also made for the cold rolled specimens parallel to the rolling plane. For these, the measured integrated intensities of selected reflections were used for determining the pole densities of austenite grains having their plane normals parallel to normal direction (ND) of the sample (Singh, 1989) and the pole density of austenite grains was expressed as

$$\frac{I_{hkl}/R_{hkl}}{\frac{1}{m}\sum I_{hkl}/R_{hkl}}$$

where I, R and m represent the integrated intensity, theoretically calculated factor and number of reflections respectively.

3. EXPERIMENTAL RESULTS

The industrially produced hot band of austenitic stainless steel was fully austenitic. The optical micrograph of the HB in the RN section near the centre (S = 0) is shown in Figure 1 and indicates mostly the elongated grains. Some recrystallised grains are also present. The dark bands in the micrograph appear to be thin sheet like bands of heavily deformed austenite grains. The average grain size measured on the section (S = 0) parallel to the rolling plane was about 7 μm.

Figure 2 shows the three dimensional orientation density distribution (i.e. ODF) of crystallites for the HB in constant ϕ_2 sections through Euler space. This ODF exhibits maxima of orientations which are given in Table 1 along with their Euler angles (ϕ_1, ϕ, ϕ_2). The main features of the texture components present in this ODF are rolling (copper-type) and recrystallisation textures. Singh, Ramaswamy and Suryanarayana (1991) have discussed the texture evolution in the present steel during hot rolling in detail and characterised the rolling texture components, which were retained, as $\{011\}\langle 112\rangle$, $\approx\{123\}\langle 634\rangle$ and $\{112\}\langle 111\rangle$ orientations and also described the orientations $\{001\}\langle 100\rangle$, RD rotated cubes $\{013\}\langle 100\rangle$, $\{012\}\langle 100\rangle$ and Goss $\langle 011\rangle\langle 100\rangle$ as the recrystallised components. The orientation elements of the retained rolling texture are distributed along an orientation tube which is inclined to constant ϕ_2 sections and extends from $\{011\}\langle 112\rangle$ at $\phi_1 = 35°$ $\phi = 45°$ and $\phi_2 = 0°$ to $\{112\}\langle 111\rangle$ at $\phi_1 = 39°$, $\phi = 66°$ and $\phi_2 = 27°$, or symmetrically equivalent and more convenient, from $\{112\}\langle 111\rangle$ at $\phi_1 = 90°$, $\phi = 35°$, and $\phi_2 = 45°$ to $\{011\}\langle 112\rangle$ at $\phi_1 = 35°$, $\phi = 45°$ and $\phi_2 = 90°$. The skeleton line of this tube also includes the orientation $\approx\{123\}\langle 634\rangle$

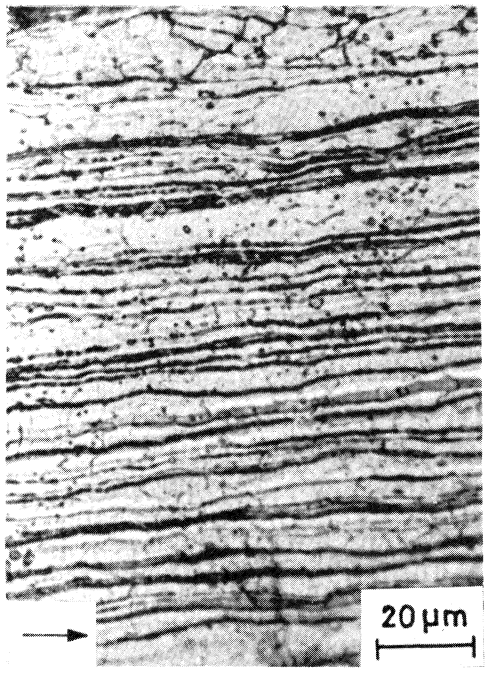

Figure 1 Optical micrograph of RN section of the hot band (HB) at centre (S = 0): arrow parallel to rolling direction.

at $\phi_1 = 59°$, $\phi = 37°$ and $\phi_2 = 63°$ and has its $\langle 110 \rangle$ fibre axis inclined ~60° from ND towards RD ($\langle 110 \rangle 60°$ND). On the other hand, the components of the recrystallised texture are scattered along $\langle 100 \rangle$//RD fibre which runs from cube $\{001\}\langle 100 \rangle$ to Goss $\{011\}\langle 100 \rangle$ positions for the constant $\phi_2 = 0°$ section (Figure 2). The major components of the rolling texture and the recrystallisation texture are $\{011\}\langle 112 \rangle$ and $\{001\}\langle 100 \rangle$ respectively.

Upon rolling the HB at 473 K, very limited amount of α'-martensite (about 16.0 vol.% at 90% reduction) was produced at the centre, which was not sufficient for its texture measurements (Singh, 1989).

The ND inverse pole figure densities of the selected planes [i.e. $(111)_\gamma$, $(200)_\gamma$, $(220)_\gamma$ and $(311)_\gamma$] parallel to the rolling plane of the cold rolled specimens, with increasing rolling reductions (range: 10–90%) are shown in Figure 3. Although, the pole density of the plane $(220)_\gamma$ is relatively higher than that of the other planes, it increases rapidly between the reductions 10 to 50%, and thereafter, remains more or less constant upto 80% reduction and then there is an increasing trend after 80% reduction. In contrast, the pole density of $(111)_\gamma$ remains relatively constant upto 40% reduction, and thereafter, increases to a maximum value at 80% reduction and then, there is a decreasing trend after 80% reduction. The pole densities of other two planes $(311)_\gamma$ and $(200)_\gamma$ are continuously decreasing with increasing reduction.

The three dimensional orientation density distributions (i.e. ODFs) of the HB cold rolled by 30, 50, 70 and 90% reductions, are presented in constant ϕ_2

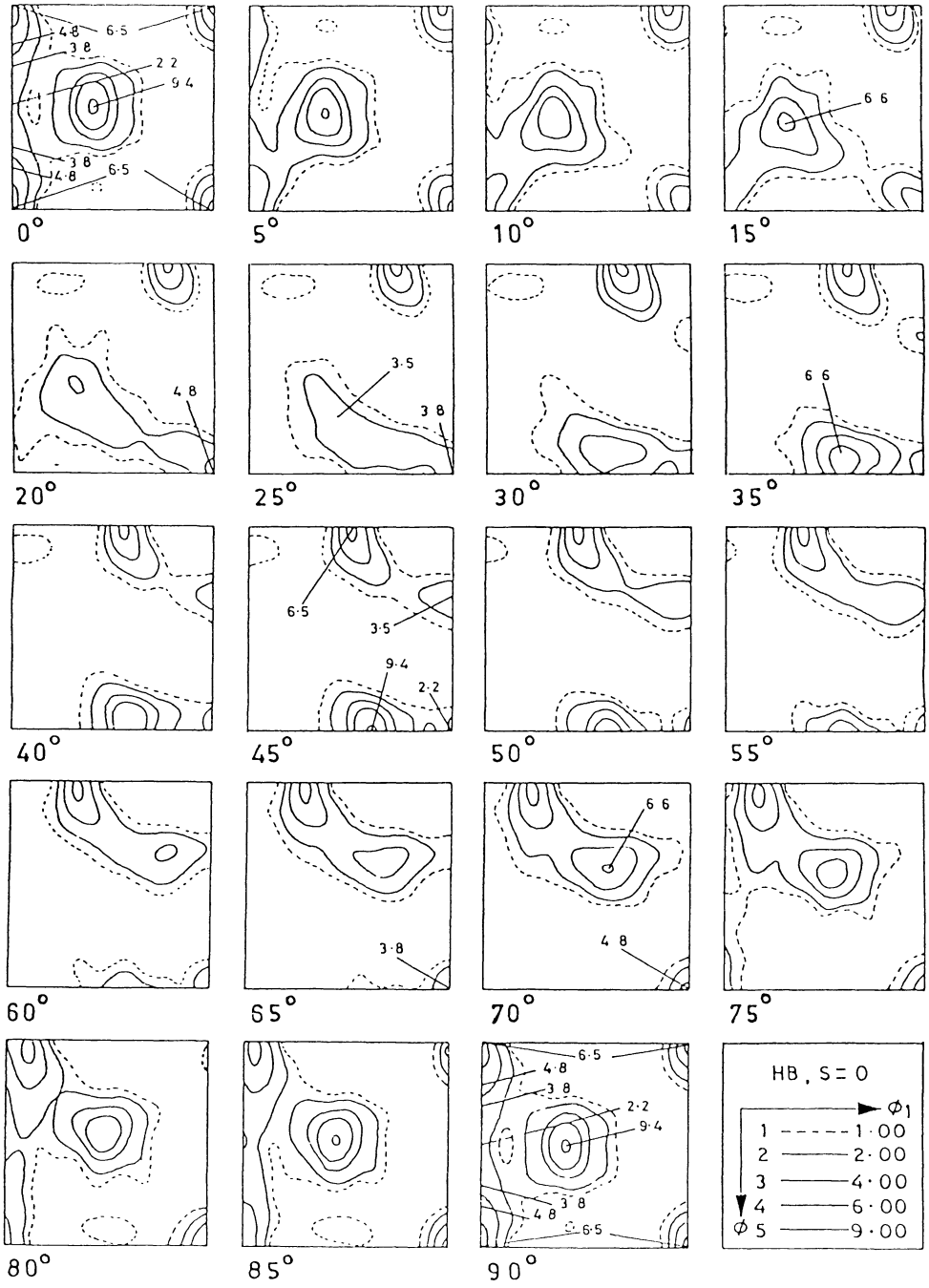

Figure 2 ODF for central level (S = 0) of the hot band (HB) in constant ϕ_2 sections. $J = 3.7$.

Table 1 Orientation density of the texture components {HKL}⟨UVW⟩ at the centre of the hot band

HKL	*UVW*	*Euler Angles*			*Orientation density*
		ϕ_1	ϕ	ϕ_2	
Retained rolling texture					
{011}	⟨112⟩	35	45	0	9.4
{134}	⟨956⟩	54	38	72	6.6
(equal to)					
{123}	⟨634⟩	59	37	63	
{112}	⟨111⟩	90	35	45	3.5
Recrystallised texture					
{001}	⟨100⟩	0	0	0	6.5
{013}	⟨100⟩	0	18	0	4.8
{012}	⟨100⟩	0	27	0	3.8
{011}	⟨100⟩	0	45	0	2.2

sections through Euler space in Figures 4(a), (b), (c) and (d) respectively. These ODF's exhibit maxima which are listed in Table 2 along with their Euler angles. While the exact orientations of the maxima are listed in the table, in the text approximate orientations are used (indicated by ≈) if the indices are clearly simpler. At low degrees of rolling [Figures 4(a) and (b)] the texture components (i.e. {011}⟨112⟩, ≈{123}⟨634⟩, ≈{112}⟨111⟩ and {011}⟨100⟩) are distributed mainly along the two limited orientation tubes in the Euler space. One of the tubes runs parallel to ϕ_1 through $\phi_2 = 0°$, $\phi = 45°$ and includes the orientations {011}⟨100⟩ at ϕ_1, ϕ, $\phi_2 = 0$, 45 and 0° and {011}⟨112⟩ at ϕ_1, ϕ, $\phi_2 = 35$, 45 and 0°. This tube has its axis ⟨110⟩//ND and the maxima in the orientation density along this tube is observed at {011}⟨112⟩ component. This maximum in orientation density at {011}⟨112⟩ is partly due to the effect of initial starting texture of the HB (Figure 2) which shows the maximum in density at {011}⟨112⟩ component. The texture index J has increased from the value of 3.7 (HB) to a value of 5.6 after cold rolling the HB by 50% reduction in thickness. Figure 5 shows the distribution of orientation densities along ⟨110⟩//ND fibre axis of the above tube. The other tube, inclined to constant ϕ_2 sections, runs from {011}⟨112⟩ at ϕ_1, ϕ, $\phi_2 = 35$, 45 and 0° to ≈{112}⟨111⟩ at ϕ_1, ϕ, $\phi_2 = 39$, 66 and 27°, or symmetrically equivalent from ≈{112}⟨111⟩ at ϕ_1, ϕ, $\phi_2 = 90$, 35 and 45° to {011}⟨112⟩ at ϕ_1, ϕ, $\phi_2 = 35$, 45, 90°. The skeleton line of this tube also includes the orientation ≈{123}⟨634⟩ at ϕ_1, ϕ, $\phi_2 = 59$, 37 and 63° and has its ⟨110⟩ fibre axis inclined ~60° from ND towards RD (⟨110⟩60°ND). Figure 6 depicts the orientation density distribution along this tube. It can be inferred from the Figures 5 and 6 that for very low degrees of rolling (e.g. ≤30%), the densities for all the texture components along the two limited tubes (i.e. ⟨110⟩//ND and ⟨110⟩60°ND fibres) increase over their whole length. The increase in density is more at {011}⟨112⟩ component than that at {011}⟨100⟩, ≈{112}⟨111⟩ and ≈{123}⟨634⟩ components. At 50% rolling reduction the densities at all texture components along ⟨110⟩//ND fibre increase very slightly and at {011}⟨112⟩ component it remains more or less constant, whereas the densities of ≈ {112}⟨111⟩ and ≈{123}⟨634⟩ components of ⟨110⟩60°ND fibre have started decreasing. At intermediate degrees of rolling (e.g. ≤70%), the orientation

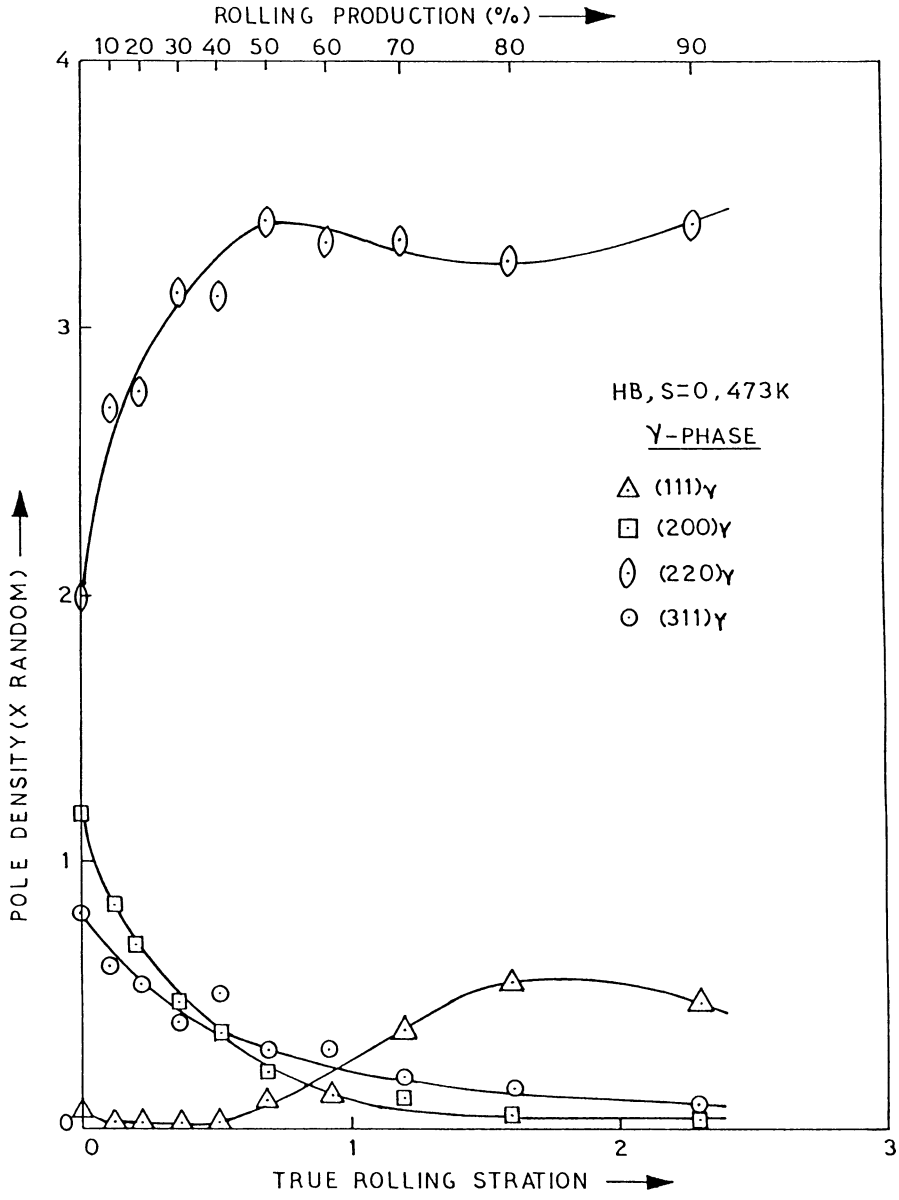

Figure 3 ND inverse pole figure data showing densities of selected planes parallel to the sheet surface of the hot band (HB) at centre (S = 0) with increasing rolling reduction at 473 K.

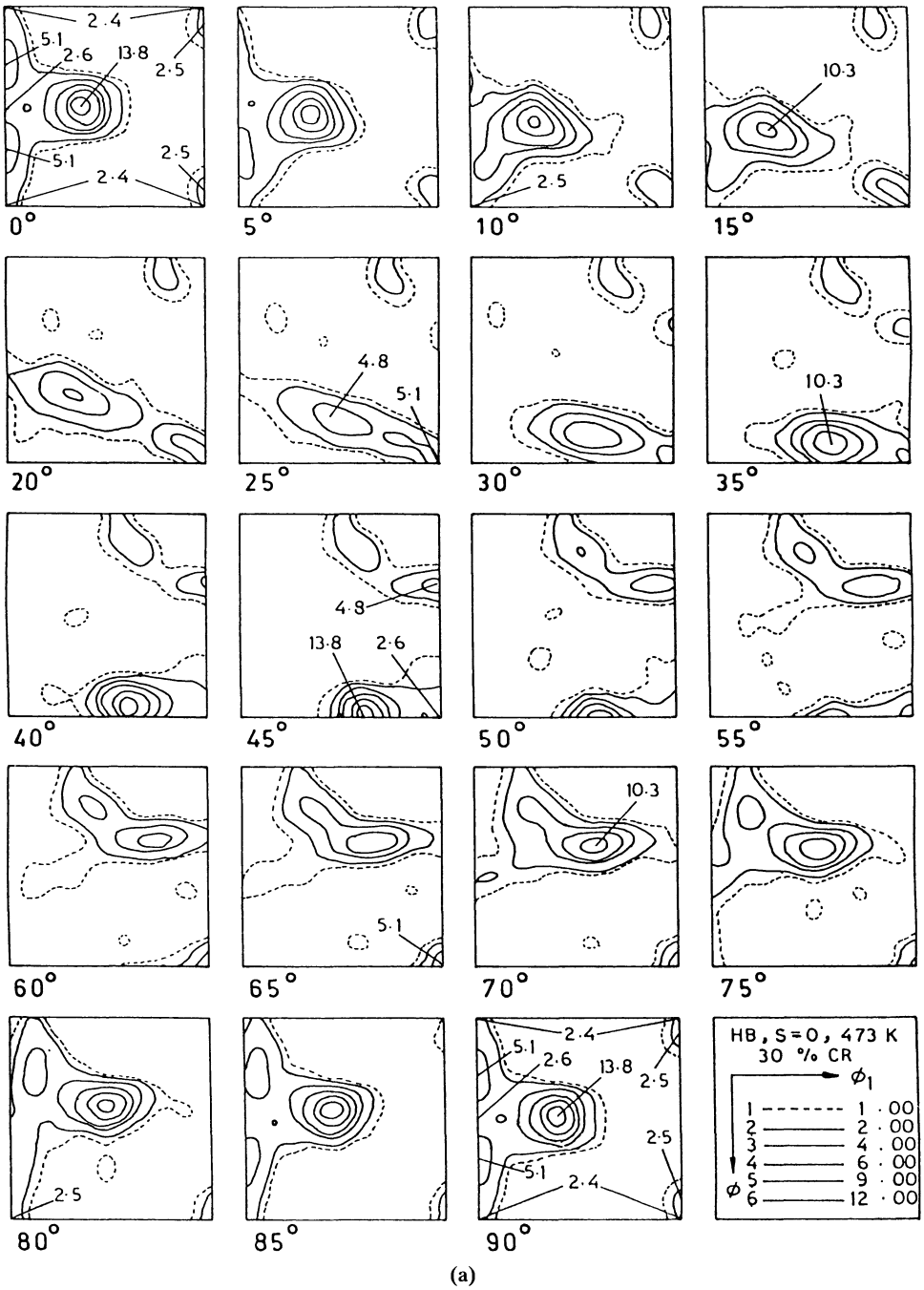

(a)

Figure 4 ODFs for central level (S = 0) of the hot band (HB) cold rolled at 473 K in constant ϕ_2 sections: (a) 30% reduction, $J = 5.6$, (b) 50% reduction, $J = 5.6$, (c) 70% reduction, $J = 5.7$ and (d) 90% reduction, $J = 6.8$.

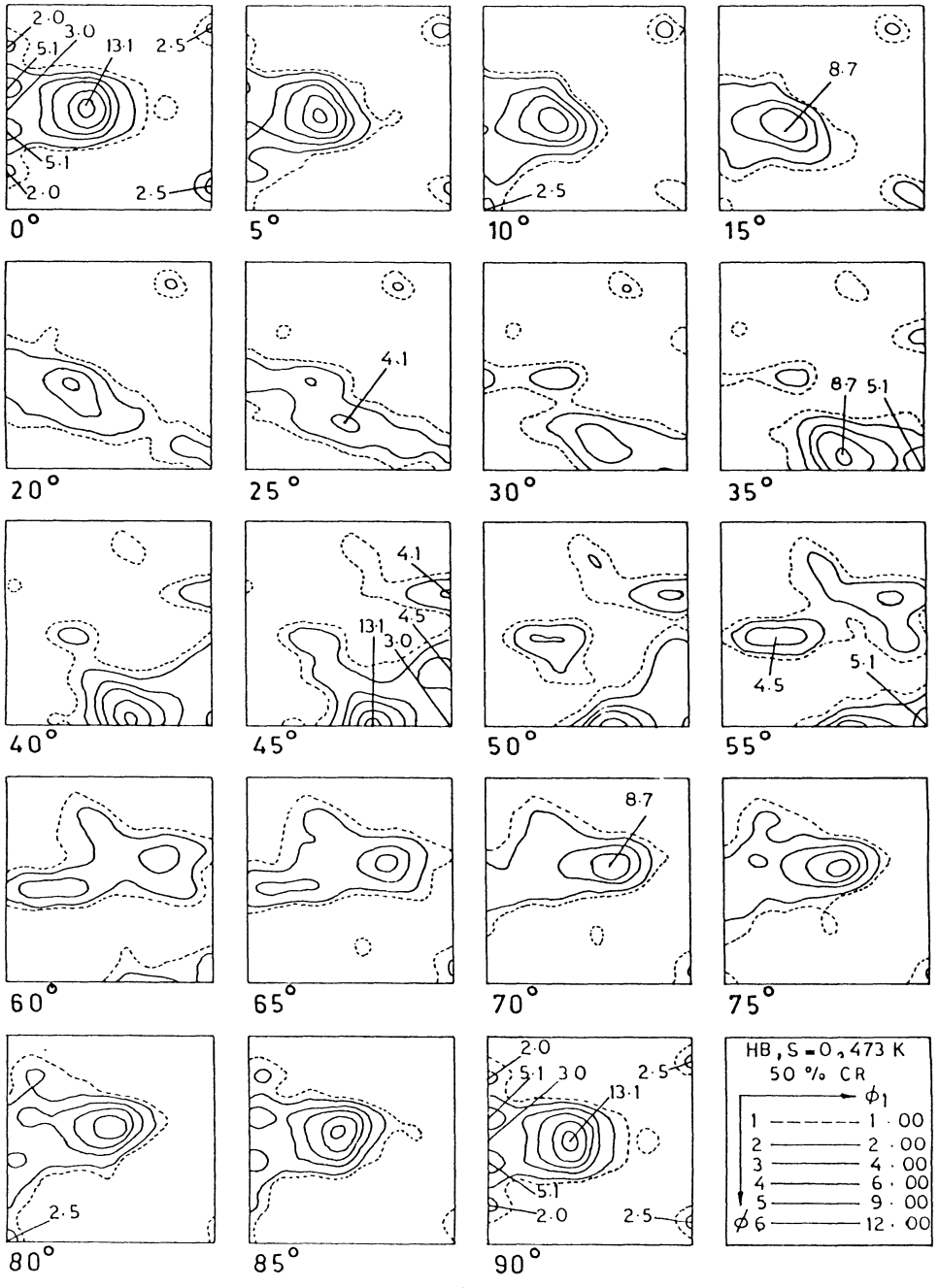

(b)

Figure 4 ODFs for central level (S = 0) of the hot band (HB) cold rolled at 473 K in constant ϕ_2 sections: (a) 30% reduction, $J = 5.6$, (b) 50% reduction, $J = 5.6$, (c) 70% reduction, $J = 5.7$ and (d) 90% reduction, $J = 6.8$.

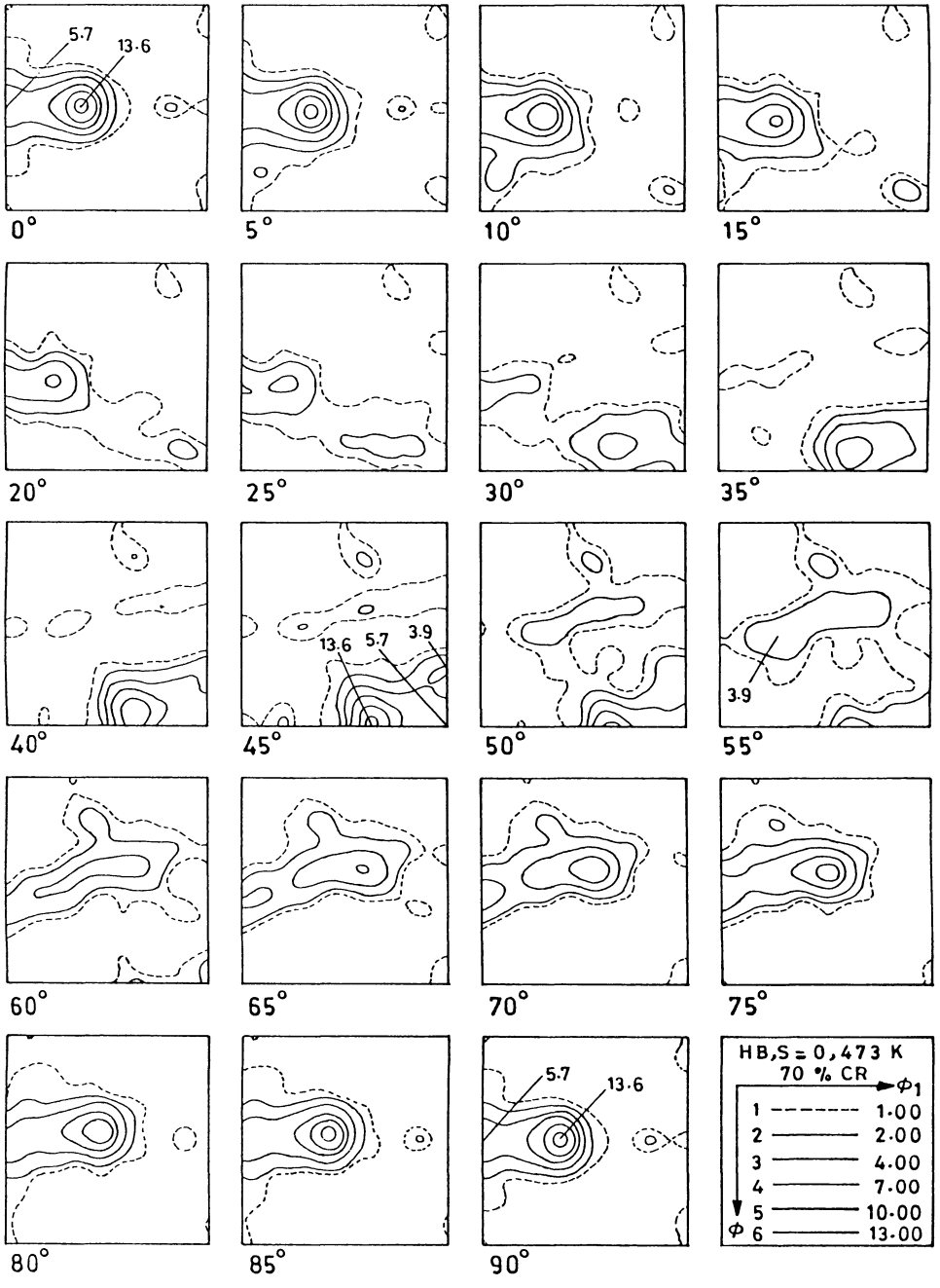

(c)

Figure 4 ODFs for central level (S = 0) of the hot band (HB) cold rolled at 473 K in constant ϕ_2 sections: (a) 30% reduction, $J = 5.6$, (b) 50% reduction, $J = 5.6$, (c) 70% reduction, $J = 5.7$ and (d) 90% reduction, $J = 6.8$.

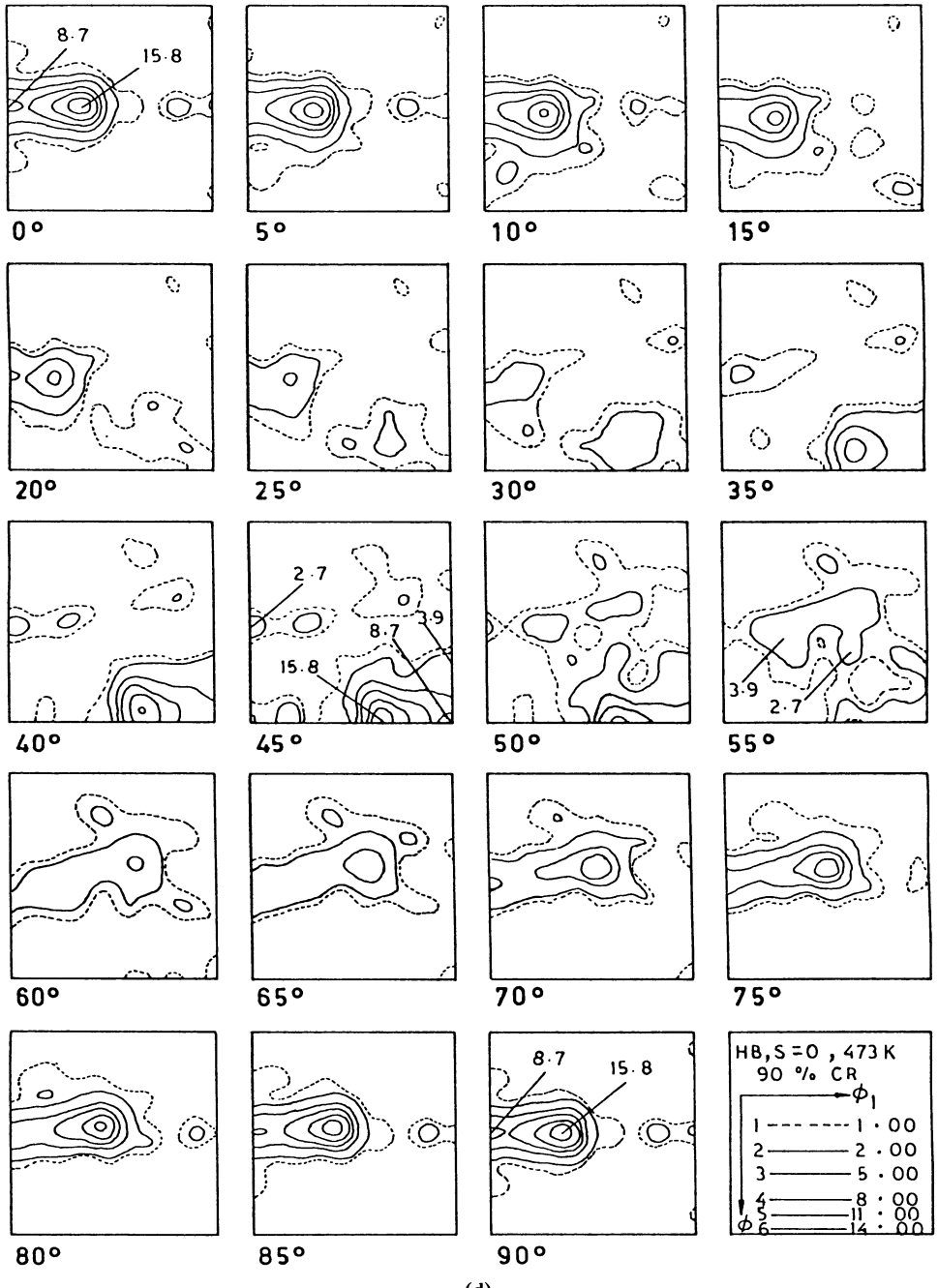

(d)

Figure 4 ODFs for central level (S = 0) of the hot band (HB) cold rolled at 473 K in constant ϕ_2 sections: (a) 30% reduction, $J = 5.6$, (b) 50% reduction, $J = 5.6$, (c) 70% reduction, $J = 5.7$ and (d) 90% reduction, $J = 6.8$.

Table 2 Orientation density of texture components of austenite at the centre of the hot band cold rolled by 30, 50, 70 and 90% reduction at 473 K

HKL	*UVW*	*Euler Angles*			*Orientation density*			
		ϕ_1	ϕ	ϕ_2	*30% CR*	*50% CR*	*70% CR*	*90% CR*
Rolling texture components								
{011}	⟨112⟩	35	45	0	13.8	13.1	13.6	15.8
{134}	⟨734⟩	49	38	72	10.3	8.7	—	—
(equal to)								
{123}	⟨634⟩	59	37	63				
{225}	⟨554⟩	90	30	45	4.8	4.1	1.6	1.3
(equal to)								
{112}	⟨111⟩	90	35	45				
{011}	⟨100⟩	0	45	0	2.6	3.0	5.7	8.7
{552}	⟨115⟩	90	74	45	1.9	—	—	—
{332}	⟨113⟩	90	65	45	1.2	5.0	4.1	4.6
{334}	⟨110⟩	0	47	45	—	—	1.5	2.7
(equal to)								
{111}	⟨110⟩	0	55	45				
{8 8 11}	⟨4 4 11⟩	90	63	45	—	4.5	3.9	3.9
(equal to)								
{111}	⟨112⟩	90	55	45				
Recrystallised texture components								
{001}	⟨100⟩	0	0	0	2.4	—	—	—
{013}	⟨100⟩	0	18	0	—	2.0	—	—
{025}	⟨100⟩	0	22	0	—	—	1.4	1.4
{012}	⟨100⟩	0	27	0	5.1	—	—	—
{023}	⟨100⟩	0	34	0	—	5.1	—	—
{0 2 11}	⟨11 2 0⟩	90	10	0	2.5	2.5	1.6	1.0

density at {011}⟨100⟩ component increases more than that at {011}⟨112⟩ component, while the densities at ≈{112}⟨111⟩ and ≈{123}⟨634⟩ components of ⟨110⟩60°ND fibre have decreased considerably. At high degrees of rolling (e.g. 90%) the orientation densities for all texture components of ⟨110⟩//ND fibre have increased considerably.

The reduction in density of ≈{112}⟨111⟩ component at ~50% reduction starts the transition of rolling texture from copper-type to brass-type. This transition is known to be caused by mechanical twinning by which the component ≈{112}⟨111⟩ twins to a position {552}⟨112⟩ near {011}⟨100⟩ component (Wassermann, 1963). The distribution of orientation densities of the component ≈{112}⟨111⟩, its twin {552}⟨115⟩, {011}⟨100⟩ and other orientations associated with further deformation by slip is shown in Figure 7 which mainly reveals the plot of orientation densities of components with a common axis ⟨110⟩//TD fibre axis against ϕ at $\phi_1 = 90°$, $\phi_2 = 45°$. The ⟨110⟩//TD fibre axis includes the component ≈{112}⟨111⟩ at $\phi = \sim 30°$, its twin at $\phi = 75°$, the component {011}⟨100⟩ at $\phi = 90°$ and the orientation {111}⟨112⟩ which is an intermediate component at $\phi = 55°$. For lower degrees of rolling, the density of the component ≈{112}⟨111⟩ increases upto ~30% reduction and then starts decreasing at about 50% reduction. Simultaneously with the reduction in the density of the component ≈{112}⟨111⟩ the orientation density of its twin position {552}⟨115⟩ starts increasing and also the twin orientation {552}⟨115⟩ has shifted its position

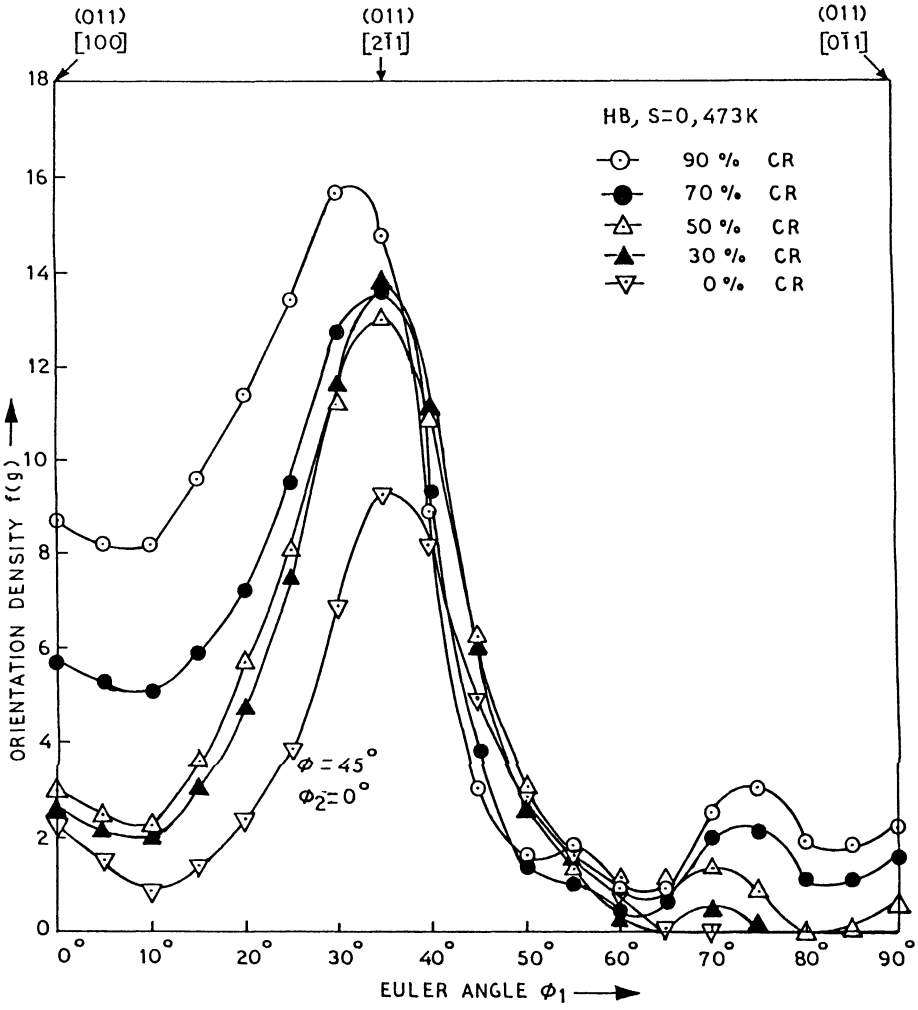

Figure 5 Orientation densities along ⟨110⟩//ND fibre of the orientation tube at the centre level (S = 0) of the hot band (HB) cold rolled by 0, 30, 50, 70 and 90% reductions at 473 K.

towards the orientation {332}⟨113⟩ at $\phi = 65°$, whereas there is very little increase in the density of the component {011}⟨100⟩. On further deformation the density of the component {332}⟨113⟩ decreases (e.g. 70% reduction) and then increases (e.g. 90% reduction), while that of the component {011}{100} progressively increases. In the same deformation range (e.g. 70–90%), an increase in the density of the component {111}⟨110⟩ has also been detected [Figures 4(c) and (d)].

Furthermore, it is clearly visible from the ODFs for HB cold rolled by 0, 30 and 50% reductions [Figures 2, 4(a) and 4(b)] that the initial scattering of the cube orientation {001}⟨100⟩ towards Goss orientation {011}⟨100⟩ in ϕ direction at $\phi_1 = \phi_2 = 0°$, has started shrinking towards the component {011}⟨100⟩ with

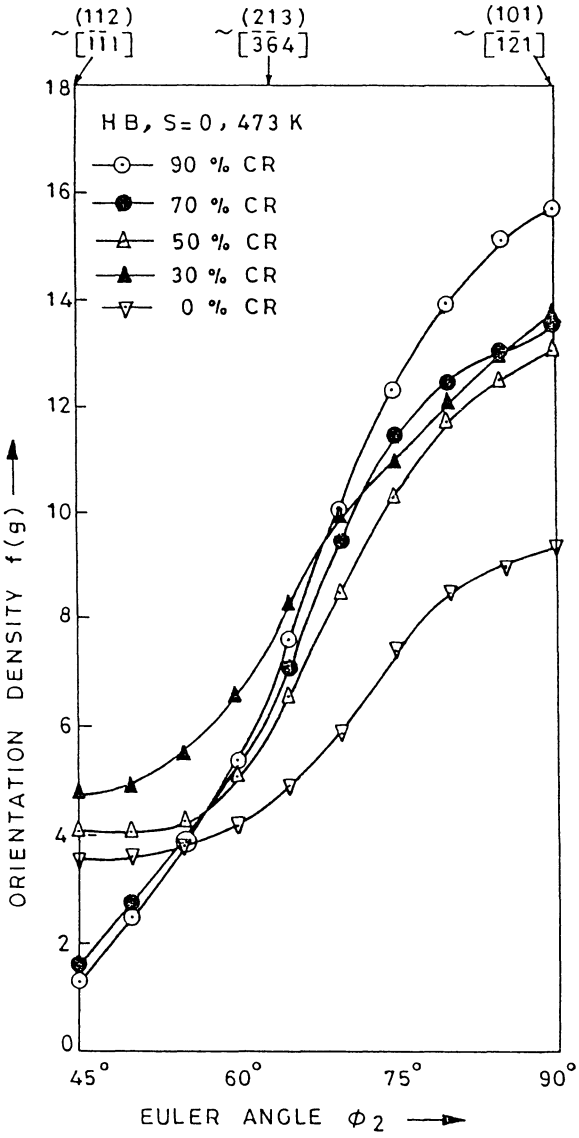

Figure 6 Orientation densities along ⟨110⟩60°ND fibre of the orientation tube at the centre level (S = 0) of the hot band (HB) cold rolled by 0, 30, 50, 70 and 90% reductions at 473 K.

increasing deformation and also there is a decrease in the density of the cube orientation with deformation.

4. DISCUSSION

The microstructure [Figure (1)] at the centre of the HB reveals the presence of deformed as well as recrystallised grains. Further, the interior layers of the HB

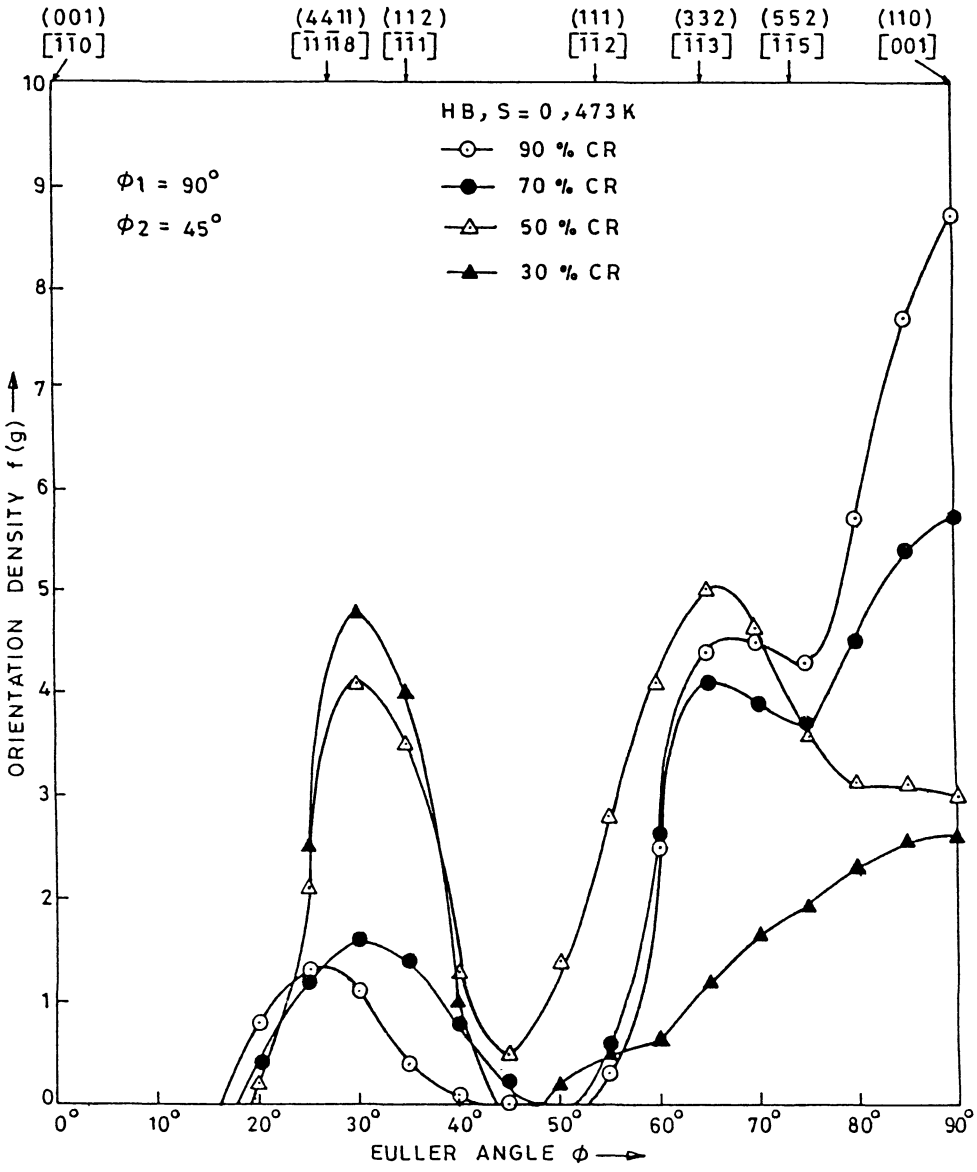

Figure 7 Orientation densities along ⟨110⟩//TD fibre at the centre level (S = 0) of the hot band (HB) cold rolled by 30, 50, 70 and 90% reductions at 473 K.

retain considerably a deformation structure. The ODF analysis of the HB also indicates the presence of textural elements of both the retained rolling textures (i.e. copper-type) and recrystallisation texture (i.e. cube and RD rotated cubes). The ⟨110⟩60°ND fibre of the copper-type texture extends from ≈{112}⟨111⟩ through the region of ≈{123}⟨634⟩ to the orientation {011}⟨112⟩ with a maximum at {011}⟨112⟩ and minimum at ≈{112}⟨111⟩. The recrystallised

texture components exhibits a scattering from cube position $\{001\}\langle 100\rangle$ towards Goss position $\{011\}\langle 100\rangle$ along with other elements of RD rotated cubes (i.e. $\{013\}\langle 100\rangle$ and $\{012\}\langle 100\rangle$). All the evidences (i.e. the presence of deformed grains and copper-type texture as well as some recrystallised grains and recrystallised texture) indicate that the HB is partially recrystallised by the process of dynamic recrystallisation during hot rolling (Singh, Ramaswamy and Suryanarayana, 1991).

The results of the ODFs analysis of the deformed austenite at the centre of the HB cold rolled at 473 K show that at low degrees of rolling ($\leqslant$50%), the observed texture components are distributed along the two limited orientation tubes. The first tube with its fibre axis $\langle 110\rangle$//ND stretches along ϕ_1 at $\phi_2 = 0°$ and $\phi = 45°$ and includes the orientations $\{011\}\langle 110\rangle$ at $\phi_1 = \phi = \phi_2 = 0$, 45 and 0° and $\{011\}\langle 112\rangle$ at $\phi_1 = \phi = \phi_2 = 35$, 45 and 0°. The other tube inclined to constant ϕ_2 sections runs through the Euler space from $\{225\}\langle 554\rangle$ ($\approx\{112\}\langle 111\rangle$) at ϕ_1, ϕ, $\phi_2 = 90$, 30 and 45° over $\approx\{123\}\langle 634\rangle$ at ϕ_1, ϕ, $\phi_2 = 59$, 37 and 63°, to $\{011\}\langle 112\rangle$ at ϕ_1, ϕ, $\phi_2 = 35$, 45 and 90° and has its fibre axis $\langle 110\rangle$ inclined ~60° from ND towards RD. The orientation element $\{011\}\langle 112\rangle$ is at the intersection point of the above two limited tubes and has the highest density amongst all the texture components. The exceptional high density of $\{011\}\langle 112\rangle$ component is partly due to the effect of starting texture of the HB (Figure 2) which shows the highest density of the orientation $\{011\}\langle 112\rangle$ and partly due to the flow of orientations of the scattered zone between the cube components $\{001\}\langle 100\rangle$ at ϕ_1, ϕ, $\phi_2 = 0$, 0 and 0° and Goss component $\{011\}\langle 100\rangle$ at ϕ_1, ϕ, $\phi_2 = 0$, 45 and 0°, along the line parallel to ϕ at $\phi_1 = \phi_2 = 0°$ from the cube to Goss component (i.e. metastable orientation) and then along the line parallel to ϕ_1 at $\phi = 45°$ and $\phi_2 = 0°$, from Goss to the component $\{011\}\langle 112\rangle$ (i.e. stable orientation) at ϕ_1, ϕ, $\phi_2 = 35$, 45 and 0°, obtained as a result of rolling. The orientation $\{225\}\langle 554\rangle$ at which the orientation tube with $\langle 110\rangle$ 60°ND fibre starts, differs by 5° from the orientation $\{112\}\langle 111\rangle$ at ϕ_1, ϕ, $\phi_2 = 90$, 35 and 45° and by 3° from the theoretically calculated orientation $\{4\,4\,11\}\langle 11\,11\,8\rangle$ at ϕ_1, ϕ, $\phi_2 = 90$, 27 and 45° by Dillamore, Butler and Green (1968) for Taylor type deformation. An increase in orientation densities for all texture components of the two limited tubes i.e. $\langle 110\rangle$//ND and $\langle 110\rangle$60°ND (Figures 5 and 6) occurs with increasing strain (e.g. $\leqslant$30% reduction). All these evidences suggest that the development of rolling textures at low degree of rolling ($\leqslant$50%) agrees fairly well with the predictions of Taylor model (Dillamore, Butler and Green, 1968).

At 50% rolling reduction, the decrease in the otherwise stable $\approx\{112\}\langle 111\rangle$ orientation marks the beginning of mechanical twinning (Wassermann, 1963) whereby the orientation $\approx\{112\}\langle 111\rangle$ undergoes mechanical twinning during rolling to form $\{552\}\langle 115\rangle$ at ϕ_1, ϕ, $\phi_2 = 90$, 75 and 45°. Wassermann (1963) has indicated that the twinning is the most favourable deformation process which causes the beginning of transition of the rolling texture from copper to brass-type. But instead of rotating to the $\{011\}\langle 100\rangle$ position and from there finally rotating to $\{011\}\langle 112\rangle$ on further rolling, the twin orientation $\{552\}\langle 115\rangle$ rotates in the opposite direction towards $\{111\}\langle 112\rangle$ on favourable slip system. The change in the orientation densities of the components $\approx\{112\}\langle 111\rangle$, twin $\{552\}\langle 115\rangle$, Goss $\{011\}\langle 100\rangle$ and other orientations obtained as a result of further deformation (Figure 7) illustrates clearly that the reverse rotation of the twin orientation $\{552\}\langle 115\rangle$ towards $\{111\}\langle 112\rangle$ at ϕ_1, ϕ, $\phi_2 = 90$, 55 and 45° occurs. These

orientation elements are mainly distributed along a fibre axis ⟨110⟩//TD which includes the orientation ≈{112}⟨111⟩ at $\phi = \sim 30°$, the twin {552}⟨115⟩ at $\phi = 75°$, the Goss component {011}⟨100⟩ at $\phi = 90°$, the orientation {111}⟨112⟩ at $\phi = 55°$ and the orientation {332}⟨113⟩ at $\phi = 65°$.

It has been reported by TEM studies of the microstructures in rolled polycrystalline 70–30 brass (Duggan *et al.*, 1978) and silver (Pospiech *et al.*, 1975) that twinning becomes an important deformation mechanism at certain strain level but instead of normal rotation of the twin component {552}⟨115⟩ towards {011}⟨100⟩, an abnormal rotation of the twin-matrix lamellae towards {111}⟨112⟩ position occurs. The orientation {111}⟨112⟩ is a position of the twin planes parallel to the rolling plane. The results of ODF analysis (Figure 7) where the twin orientation {552}⟨115⟩ at intermediate degrees of rolling ($\geqslant 50\%$), shifts to lower ϕ angles instead of rotating towards {011}⟨100⟩ position, prove that a rotation towards {111}⟨112⟩ position takes place, whereas the orientation density of the orientation {011}⟨100⟩ remains more or less constant (i.e. rather increases very slightly).

This abnormal rotation towards {111}⟨112⟩ is mainly due to the preferred slip on slip planes parallel to the coherent twin boundaries of the twin lamellae. In metals of low SFE, the normal slip on the slip planes of highest critical resolved shear stress, is severely limited mainly because of the very small width of the twin lamellae (Peissker, 1965). Further, the shear stress for the abnormal slip starts decreasing and finally becomes zero as the twin-parent lamellae become oriented with the rolling plane, and ultimately the abnormal rotation stops and, as detected in Figure 7, the statistical maxima of the rotated orientations is observed near {332}⟨113⟩, which is 10° away from {111}⟨112⟩ position. The rotation of the matrix orientation ≈{112}⟨111⟩ towards {111}⟨112⟩ could not be observed in the ODF results (Figure 7) mainly because the obtained ODF is the reduced ODF. However, Hirsch, Virnich and Lücke (1981) have reported the rotation of matrix orientation towards {111}⟨112⟩ position in 70–30 brass with the help of complete ODF.

Besides the component {332}⟨113⟩ at intermediate degree of rolling, an orientation near {111}⟨110⟩, also with {111} plane nearly parallel to the rolling plane appears. Since {111}⟨110⟩ develops simultaneously with the {332}⟨113⟩, it can be assumed that this position is formed by the preferential slip on one of the two active slip systems parallel to the twin boundary that rotates the twin component {552}⟨115⟩ and other possible twin orientation of ≈{123}⟨634⟩ component. The twin of ≈{123}⟨634⟩ component is symmetrically equivalent to ≈{123}⟨634⟩ position. This causes the rotation of the preferred slip direction parallel to the rolling plane.

Since the rotated twin-matrix lamellae finally no longer contribute to deformation process by slip, on further rolling shear bands form in the highly unstable structure of aligned twin-matrix lamellae. Formation of shear bands has been observed by many investigators (Duggan *et al.*, 1978; Hatherly, 1978; Blicharski and Gorczyca, 1978; Wakefield and Hatherly, 1981) in their TEM studies. According to these investigators shear bands usually form at 35° to the rolling plane and the formation of these bands is mainly responsible for the decrease of {111} orientations at high degree of rolling (i.e. $\geqslant 70\%$). Further, such a rotation by ±35° around TD would lead {111}⟨112⟩ (i.e. observed orientation {332}⟨113⟩) to {011}⟨100⟩ position at ϕ_1, ϕ, $\phi_2 = 90$, 90 and 45°, and to ≈{112}⟨111⟩ position at ϕ_1, ϕ, $\phi_2 = 90$, 20 and 45°, and also the orientation

$\{111\}\langle 110\rangle$ to a position in between $\approx\{123\}\langle 634\rangle$ and $\{011\}\langle 112\rangle$ positions. The observations, an increase in the density of $\{011\}\langle 100\rangle$ component and the shifting of $\approx\{112\}\langle 111\rangle$ component towards lower ϕ values after intermediate degree (i.e. 70% reduction) and high degree (i.e. 90% reduction) of rolling (Figure 7) and also an increase in the orientation density of $\{011\}\langle 112\rangle$ component (Figure 6) after 90% reduction, establish the formation of shear bands in the above deformation range (i.e. intermediate and high degrees of rolling). Further, the cyclic variation in the orientation density of $\{332\}\langle 113\rangle$ component after 50% reduction indicates a competition between mechanical twinning and the associated abnormal slip on one hand and shear bands formation in the rotated twin-matrix lamellal on the other. Twinning and abnormal rotation cause an increase whereas the shear bands formation leads to a decrease in the density of $\{332\}\langle 113\rangle$ component. At 90% reduction, the observation of highest density at $\{011\}\langle 112\rangle$ component also indicates that normal slip is re-occurring in the crystallites of the shear bands and sharpens the brass-type rolling texture (i.e. $\langle 110\rangle$//ND orientation tube).

The variation in the ND inverse pole figure densities of selected planes parallel to rolling plane of the cold rolled HB, with increasing reduction (Figure 3) can be correlated with ODF results. The $\{220\}_\gamma$ reflection may be considered as representative of the orientations $\{011\}\langle 100\rangle$ and $\{011\}\langle 112\rangle$. The twin rotated orientations $\{332\}\langle 113\rangle$ and $\{111\}\langle 110\rangle$ approximate the reflection $\{111\}_\gamma$ whereas the reflection $\{311\}_\gamma$ represents approximately $\approx\{112\}\langle 111\rangle$ component. At low degrees of rolling (<50% reduction), the deformation is occurring primarily by normal octahedral slip process which causes the flow of recrystallised texture components of the HB from cube position $\{001\}\langle 100\rangle$ through Goss orientation $\{011\}\langle 100\rangle$ to $\{011\}\langle 112\rangle$ position and simultaneously there is an increase in the density of $\approx\{112\}\langle 111\rangle$ and $\approx\{123\}\langle 634\rangle$ components. The rapid increase in the density of $\{220\}_\gamma$ reflection indicates the flow of orientations due to normal slip. The reduction in the density of $\approx\{112\}\langle 111\rangle$ component at 50% reduction establishes the occurrence of mechanical twinning and the twin $\{552\}\langle 115\rangle$-matrix lamellae get rotated towards $\{111\}\langle 112\rangle$ at intermediate degrees of rolling (i.e. $\geqslant$50% reduction). This abnormal rotation of twin-matrix lamellae finally stops near $\{332\}\langle 113\rangle$ orientation which is 10° apart from $\{111\}\langle 112\}$ and simultaneously there is the development of $\{111\}\langle 110\rangle$ orientation. The increase in the pole density of $\{111\}_\gamma$ reflection to a maximum value at about 80% reduction represents this stage (i.e. the orientations $\{332\}\langle 113\rangle$ and $\{111\}\langle 110\rangle$). The formation of the shear bands in the rotated twin-matrix lamellae causes the destruction of the orientations $\{332\}\langle 113\rangle$ and $\{111\}\langle 110\rangle$ and hence decreases the pole density of $\{111\}_\gamma$ reflection and finally rotate these orientations to $\{011\}\langle 100\rangle$ and near $\{011\}\langle 112\rangle$ positions. In addition, again normal slip occurs in the grains of shear bands which sharpens the texture components $\{011\}\langle 112\rangle$ and $\{011\}\langle 100\rangle$ of the brass-type rolling texture (i.e. $\langle 110\rangle$//ND orientation tube) as reflected by the increasing tendency of the pole density of $\{220\}_\gamma$ reflection after 80% rolling reduction.

5. CONCLUSIONS

(i) At very low degree of rolling (i.e. 30% reduction), the texture consists of two limited fibres i.e. $\langle 110\rangle$//ND and $\langle 110\rangle$60°ND. The $\langle 110\rangle$//ND fibre runs

from {011}⟨100⟩ to {011}⟨112⟩ and the ⟨110⟩60°ND fibre stretches from ≈{112}⟨111⟩ through ≈{123}⟨634⟩ to {011}⟨112⟩. The development of these two limited fibres agrees to the predictions of Taylor model based on normal octahedral slip.

(ii) At low degree of rolling (i.e. 50% reduction) mechanical twinning leads to the reduction of ≈{112}⟨111⟩ component and the formation of twin component {552}⟨115⟩ in form of the fine twin-matrix lamellae.

(iii) At the intermediate degrees of rolling (i.e. ≥50% reduction) slip is preferred on planes parallel to the twin boundaries of the fine twin lamellae, leading to an abnormal rotation of twin-matrix lamellae into {332}⟨113⟩ and {111}⟨110⟩ and finally this abnormal rotation stops when the slip plane becomes parallel to the rolling plane.

(iv) At intermediate (i.e. 70% reduction) and high (i.e. 90% reduction) degrees of rolling, the formation of shear bands in the rotated twin-matrix regions changes the orientations {332}⟨113} and {111}⟨110⟩ near to {011}⟨100⟩ and {011}⟨112⟩ positions respectively.

(v) At high degree of rolling (i.e. 90% reduction) the re-establishment of homogeneous slip in the fine grains of shear bands causes sharpening of the brass-type rolling texture by the rotation of {011}⟨100⟩ component to {011}⟨112⟩ component.

ACKNOWLEDGEMENTS

The authors would like to express their gratitude to the management of RDCIS, SAIL, Ranchi for according the permission to publish this work.

References

Alam, R., Mengelberg, H. D. and Lücke, K. (1967). *Z. Metallkde.* **58,** 867.
Bacroix, B. and Jonas, J. J. (1988). In *Proceedings ICOTOM8: Textures of Materials.* Ed. J. S. Kallend and G. Gottstein, The Metallurgical Society, Inc. 403.
Blicharski, M. and Gorczyca, S. (1978). *Metal Sci.* **12,** 303.
Bunge, H. J. (1969). *Mathematische Methoden der Texturanalyse,* Akademie-Verlag, Berlin.
Bunge, H. J. (1970). *Krist. Tech.* **5,** 145.
Bunge, H. J. (1971). *Krist. Tech.* **6,** 429.
Bunge, H. J. (1982). *Texture Analysis in Materials Science,* Butterworths, London.
Bunge, H. J. and Haessner, F. (1968). *J. Appl. Phys.* **39,** 5503.
Bunge, H. J. and Tobisch, J. (1968). *Z. Metallkde,* **59,** 471.
Davies, G. J., Kallend, J. S. and Ruberg, T. (1973). In *Proceedings ICOTOM3: 3^e Colloque Europeen Sur Les Textures de Deformation et de Recristallisation des Me'taux et Leur Applications Industrielles.* Ed. R. Penelle, Societe' Francaise de Metallurgie, Pont-a-Mousson, 299.
Dillamore, I. L. and Katoh, H. (1971). BISRA Open Report, MG/39/71.
Dillamore, I. L. and Katoh, H. (1974). *Metal Sci.* **8,** 21.
Dillamore, I. L., Butler, E. and Green, D. (1968). *Metal Sci.* **2,** 161.
Duggan, B. J., Hatherly, M., Hutchinson, W. B. and Wakefield, P. T. (1978). *Metal. Sci.* **12,** 34.
Fargette, B. and Whitwham, D. W. (1976). *Me'm. Sci. Rev. Me'tall.* **73,** 197.
Goodman, S. R. and Hu, H. (1964). *Trans. Met. Soc. AIME.* **230,** 1413.
Grewen, J. and Wassermann, G. (1955). *Acta Met.* **3,** 354.
Grewen, J., Noda, T. and Sauer, D. (1977). *Z. Metallkde.* **68,** 260.

Hatherly, M. (1978). In *Proceedings ICOTOM5: Textures of Materials,* Vol. 1. Ed. G. Gottstein and K. Lücke, Springer-Verlag, Berlin, 81.
Hirsch, J. and Lücke, K. (1988). *Acta Met.* **36,** 2863.
Hirsch, J., Virnich, K. H. and Lücke, K. (1981). In *Proceedings ICOTOM6: Textures of Materials,* Vol. 1. Ed. S. Nagashima, The Iron and Steel Institute of Japan, Tokyo, 375.
Honneff, H. and Mecking, H. (1981). In *Proceedings ICOTOM6: Textures of Materials,* Vol. 1. Ed. S. Nagashima, The Iron and Steel Institute of Japan, Tokyo, 347.
Hu, H. and Cline, R. S. (1961). *J. Appl. Phys.* **32,** 760.
Hu, H. and Goodman, S. R. (1963). *Trans. Met. Soc. AIME.* **227,** 627.
Hu, H., Cline, R. S. and Goodman, S. R. (1961). *J. Appl. Phys.* **32,** 1392.
Hu, H., Sperry, P. R. and Beck, P. A. (1952). *Trans. Met. Soc. AIME.* **194,** 76.
Hutchinson, W. B., Duggan, B. J. and Hatherly, M. (1979). *Metals Tech.* **6,** 398.
Kern, R. and Bergmann, H. W. (1978). In *Proceedings ICOTOM5: Textures of Materials,* Vol. 1. Ed. G. Gottstein and K. Lücke, Springer-Verlag, Berlin, 139.
Lücke, K. (1981). In *Proceedings ICOTOM6: Textures of Materials,* Vol. 1. Ed. S. Nagashima, The Iron and Steel Institute of Japan, Tokyo, 14.
Malin, A. S. and Hatherly, M. (1979). *Metal Sci.* **8,** 463.
Peissker, E. (1965). *Z. Metallkde.* **56,** 155.
Pospiech, J. and Lücke, K. (1975). *Acta Met.* **23,** 997.
Pospiech, J., Truszkowski, W., Jura, J. and Krol, J. (1975). In *Proceedings ICOTOM4: Texture and Properties of Materials.* Ed. G. J. Davies, I. L. Dillamore, R. C. Hudd and J. S. Kallend, The Metals Society, Cambridge, 23.
Schulz, L. G. (1949). *J. Appl. Phys.* **20,** 1030.
Singh, C. D. (1989). Ph.D. Thesis, Banaras Hindu University, Varanasi, India.
Singh, C. D., Ramaswamy, V. and Suryanarayana, C. (1991). *Textures and Microstructures* **13,** 227.
Truszkowski, W., Pospiech, J., Betzl, M. and Jura, J. (1978). In *Proceedings ICOTOM 5: Textures of Materials,* Vol. 1. Ed. G. Gottstein and K. Lücke, Springer-Verlag, Berlin, 253.
Truszkowski, W., Pospiech, J., Jura, J. and Major, B. (1973). In *Proceedings ICOTOM3: 3^{e} Colloque Europeen Sur les Textures de Deformation et de Recristallisation des Me'taux et Leur Applications Industrielles.* Ed. R. Penelle, Societe' Francaise de Metallurgie, Pont-a-Mousson, 235.
Van Houtte, P. (1978a). *Acta Met.* **26,** 591.
Van Houtte, P. (1978b). In *Proceedings ICOTOM5: Textures of Materials,* Vol. 1, Ed. G. Gottstein and K. Lücke, Springer-Verlag, Berlin, 347.
Van Houtte, P. (1981). In *Proceedings ICOTOM6: Textures of Materials,* Vol. 1, Ed. S. Nagashima, The Iron and Steel Institute of Japan, Tokyo, 428.
Van Houtte, P. and Aernoudt, E. (1976). *Mat. Sci. Engg.* **23,** 11.
Virnich, K. H. and Lücke, K. (1978). In *Proceedings ICOTOM5: Textures of Materials,* Vol. 1. Ed. G. Gottstein and K. Lücke, Springer-Verlag, Berlin, 397.
Wakefield, P. and Hatherly, M. (1981). *Metal Sci.* **3,** 109.
Wassermann, G. (1963). *Z. Metallkde.* **54,** 61.
Wassermann, G. and Grewen, J. (1962). *Texturen Metallischer Werkstoffe.* Springer-Verlag, Berlin.